

Soft Matter

Accepted Manuscript



This is an *Accepted Manuscript*, which has been through the Royal Society of Chemistry peer review process and has been accepted for publication.

Accepted Manuscripts are published online shortly after acceptance, before technical editing, formatting and proof reading. Using this free service, authors can make their results available to the community, in citable form, before we publish the edited article. We will replace this *Accepted Manuscript* with the edited and formatted *Advance Article* as soon as it is available.

You can find more information about *Accepted Manuscripts* in the [Information for Authors](#).

Please note that technical editing may introduce minor changes to the text and/or graphics, which may alter content. The journal's standard [Terms & Conditions](#) and the [Ethical guidelines](#) still apply. In no event shall the Royal Society of Chemistry be held responsible for any errors or omissions in this *Accepted Manuscript* or any consequences arising from the use of any information it contains.



Soft Matter
ARTICLE

The component groups structure of DPPC bilayers obtained by specular neutron reflectometry[†]

Received 00th January 20xx,
Accepted 00th January 20xx

Michal Belička,^{a,b,c,*} Yuri Gerelli,^c Norbert Kučerka^{b,d} and Giovanna Fragneto^c

DOI: 10.1039/x0xx00000x

www.rsc.org/

Specular neutron reflectometry was measured on a floating bilayer system consisting of 1,2-dipalmitoyl-d62-*sn*-glycero-3-phosphocholine deposited over a 1,2-dibehenoyl-*sn*-glycero-3-phosphocholine bilayer at 25 and 55 °C. The internal structure of lipid bilayers was described by a one-dimensional neutron scattering length density profile model, originally developed for the evaluation of small-angle scattering data. The reflectivity data from the supported bilayer were evaluated separately and used further as constraints in modeling the floating bilayer reflectivity curves. The model reflectivity curves successfully describe the experimental reflectivities of the supported bilayer in gel phase and the floating bilayer system in the liquid-crystalline phase. The results yield internal structure of a deposited and a floating bilayer on the level of component groups of lipid molecules. The obtained structure of the floating d62-diC16:0PC bilayer displays high resemblance of the bilayer structure in the form of unilamellar vesicles. At the same time however, the results show differences in comparison to unilamellar vesicle bilayers, most likely due to the undulations of supported bilayers.

Introduction

Biological lipid membranes represent natural boundaries in living cells, where they define intra- and intercellular compartments containing specific biochemical environments. Hydrocarbon chains located in the centre of biomembranes form a hydrophobic barrier with different rates of penetration for water, ions and small molecules. Simultaneously, they serve as docking platforms for various biological macromolecules and influence their functions.¹ All physico-chemical properties of biomembranes are altered by the bilayer composition and surrounding medium properties (temperature, pressure, composition, etc.). In principle, they are the result of complicated lipid-lipid, lipid-environment and lipid-macromolecule interactions. Molecular arrangement inside lipid biomembranes at an equilibrated state reflects these interactions. Therefore, each experimental technique capable of probing the biomembrane internal structure provides a very valuable tool for the study of such complex dynamical systems. This is the case of specular neutron reflectometry (SNR).²

A wide variety of lipids and other molecules present in natural biological membranes makes structural studies difficult due to their complicated composition, therefore artificial lipid bilayers with a controlled composition are preferred as simpler biomembrane models. The utilized form of lipid bilayers depends on the requirements of a given experimental

technique and on the object of interest in a given experiment. Therefore each form of lipid bilayers yields some advantages or drawbacks according to the posed goals. Multi- and unilamellar vesicles are primarily used in neutron and/or X-ray diffraction and small-angle scattering experiments, and can be easily prepared in several ways.^{3–5} From the point of view of scattering experiments they are an excellent kind of the bilayer form for structural studies of single or multicomponent lipid systems.^{6–10} On the other side they are not ideal forms for investigations of the influences of large biomacromolecules (e.g. polypeptides, nucleic acids, proteins) on lipid bilayers as in the case of unilamellar vesicles it is difficult to avoid their mutual interactions, whereas in multilamellar vesicles there are restrictions given by the interlamellar water spacing. The stacks of aligned fully hydrated bilayers are used as well. They are usually prepared from organic solvent-lipid solutions deposited on solid substrates, and brought into contact with water after solvent removal.^{11,12} The stacks prepared in this way consist of hundreds of bilayers, hence, when considered as one-dimensional crystals, they are bilayer arrangements very well-suited primarily for diffraction techniques and allow model free investigations of their inner structure.^{12–15} Their disadvantage is, similarly to multilamellar vesicles, that the investigations of interactions of larger macromolecules with lipid bilayers are limited by the interlamellar distances in the stacks and the *in situ* control of water environment is very limited. One way how to avoid the above mentioned complications is application of SNR to a single supported bilayer^{16–18} or a bilayer floating over a supported one^{2,19,20} or a chemically grafted bilayer²¹ at the solid/water interface. The surface of the solid substrate (usually silicon) can be hydrophilic (e.g. with a SiO₂ layer) or hydrophobic (e.g. with an Au layer). Whereas a supported membrane interacts with the solid surface, hence its fluidity and fluctuations may not be in a biologically relevant state, the floating bilayer interacts with

^a Faculty of Pharmacy, Comenius University, SK-832 32 Bratislava, Slovakia.

^b Institute of Molecular Biosciences, Biophysics Division, University of Graz, Austria.

^c Institut Laue-Langevin, FR-38042 Grenoble Cedex 9, France.

^d Frank Laboratory of Neutron Physics, Joint Institute for Nuclear Research, Dubna, Moscow Region, 141980, Russia

* Corresponding author at: Department of Physical Chemistry of Drugs, Faculty of Pharmacy, Comenius University, Odbojárov 10, SK-832 32 Bratislava, Slovakia
Email address: belicka@fpharm.uniba.sk (M. Belička)

[†] Dedicated to Professor Pavol Balgavý on the occasion of his 70th birthday.

COMMUNICATION

Journal Name

the supported one in the same way as bilayers in multilamellar vesicles or in stacks, and thus it can be considered as a more suitable biomembrane model.

SNR has proved to be a powerful and reliable method for the structural investigation of nanometer-scale films located at media interfaces (e.g. silicon/water, water/oil, water/air). In principle, it utilizes the wave properties of neutrons and the fact they are reflected and refracted on the common boundary of two media with different neutron scattering length densities (NSLD). Thermal and cold neutrons, produced by nuclear reactors or spallation sources, are exceptionally well suited for these studies as they deeply penetrate samples without their destruction, in contrast to X-rays. In combination with the well-known contrast variation technique²² they allow to detect structures at the level of the Ångström. In a SNR experiment the measured reflectivity, R , is given by the ratio of the reflected beam to the incident beam intensities and it captures the (averaged) internal profile of an irradiated planar structure. By SNR only the structure in the direction of transferred momentum is considered, i.e. in the direction of the bilayer normal. The inhomogeneities in the structure plane are averaged.

As for many other scattering techniques the lack of phase information in the reflected beam involves the application of a model to obtain the SLD profile. Models used for the neutron reflectometry data evaluation are usually directly based on the so-called box model,² in which the profile of a deposited structure is represented by strips (boxes) with constant composition, parameterized by their thicknesses, SLDs and the roughnesses of their borders. Particularly, in the case of lipid bilayers whole regions of the same nature like hydrocarbon chains, polar heads with intercalated water molecules or water molecules between a supported and a floating bilayer are represented by distinct homogeneous layers. The construction of a corresponding model reflectivity curve follows from basic optical principles.²³

The main aim of our work is to investigate the possibilities of a more detailed bilayer model for application in SNR studies focused on lipid bilayers. Both, a supported and a floating bilayer are represented by the scattering density profile (SDP) model which was recently successfully applied to small-angle X-ray and neutron scattering data.^{24–26} A similar model has already been applied by Shekhar *et al.*²⁷ for the evaluation of SNR on supported lipid membranes. Our floating bilayer was formed by 1,2-dipalmitoyl-d62-*sn*-glycero-3-phosphocholine with deuterated hydrocarbon chains (d62-d1C16:OPC) with main phase transition temperature 41 °C. This allowed to deposit its monolayers in the solid phase, a crucial condition for Langmuir type depositions, and to change its phase easily within a biologically relevant temperature range during the measurements. Moreover the structure of d1C16:OPC bilayers has been studied extensively by various scattering methods in the past,^{28–31} what makes them an ideal candidate for a validation of novel model. As a system of floating bilayers consists of two, in general different, bilayers, we divided the whole process of data analysis into two main parts. In the first step we studied a supported bilayer only. In the next step we applied the obtained structure of the supported bilayer as an

input for a more complicated floating bilayer system. The floating bilayer was measured at two different temperatures to compare its structure in the gel and fluid phases.

Experimental

Sample preparation

1,2-dibehenoyl-*sn*-glycero-3-phosphocholine (d1C22:OPC) and 1,2-dipalmitoyl-d62-*sn*-glycero-3-phosphocholine (d62-d1C16:OPC) were purchased from Avanti Polar Lipids (Alabaster, USA). All organic solvents were used as received from Sigma Aldrich (St Louis, USA). Fresh Milli-Q water (18 M Ω cm, named H₂O in the following) and D₂O of isotopic 99 % purity were supplied by the Institut Laue-Langevin (ILL), Grenoble. All water was degassed prior to use to avoid formation of air bubbles in the solid-liquid cells during high temperature measurements. Silicon (111) substrates in the form of 8 × 5 × 1.5 cm³ blocks with a single polished side were used as solid support for depositions. Shortly before sample preparation, the block was cleaned in chloroform, acetone and ethanol subsequently in an ultrasonic bath in each solvent for 15 minutes. Afterwards the block was exposed to ozone for 30 min and rinsed with H₂O.

The process of sample preparation was carried out in a Nima 1212D Langmuir trough (Nima Technology, Coventry, UK) filled with H₂O and cooled down to 13 °C. Monolayers at the water/air interface were prepared from chloroform lipid solutions at 1 mg/ml concentration, which were spread in small droplets on a water surface. After evaporation of the organic solvent (15 min), lipid monolayers were slowly compressed up to a lateral pressure of 40 mN m⁻¹. Langmuir-Blodgett monolayer transfers were then performed at a constant pressure. In order to prepare stable floating bilayer systems d1C22:OPC molecules were used to prepare the bilayer facing the solid support. On its top a floating bilayer composed by d62-d1C16:OPC molecules was deposited. The whole process of the floating bilayer system preparation comprised a combination of the Langmuir-Blodgett (vertical) and the Langmuir-Schaefer (horizontal) deposition techniques, as described in detail elsewhere.¹⁹ After the last deposition the silicon block was sealed in standard solid-liquid cells (provided by the ILL) without removing it from the water in order to avoid the contact of the deposited sample with air. The holder was equipped with two valves for solvent exchange and cooling system for keeping the sample at the desired temperature. The sample was prepared 24 hours before measurements and was stored at 8 °C in the cold room. A simpler adhered bilayer composed of d1C22:OPC molecules was prepared and characterized as a reference for data analysis.

Measurements

SNR measurements were performed at the Institut Laue-Langevin (Grenoble, France) at the high flux D17 reflectometer.³² The instrument was operated in time-of-flight (ToF) mode using an interval of neutron wavelengths between 2 and 18 Å and two incident angles 0.8° and 3.2°. The q range (where $q = 4\pi / \lambda \sin(\theta)$ is the momentum transfer, θ is an

Journal Name

incident and 2θ scattering angle) covered an interval from 0.005 to 0.2 \AA^{-1} . All the samples were measured in three different (*i.e.*, 100%, 50% and 0%) H₂O/D₂O mixtures (having different NSLD) and at 25 °C and 55 °C (below the main phase transition of diC22:0PC which is at 75 °C and respectively below and above this transition in d62-diC16:0PC³³). The direct experimental data obtained from the reflectometer were treated using the COSMOS routine of LAMP software package,³⁴ through which they were converted into $R(q)$ curves. Data files generated by COSMOS contain information about the experimental q -resolution and this was used during data analysis.

Data analysis

Reflectometry principles. The neutron reflectivity $R(\bar{q})$, where \bar{q} is transferred momentum, is defined as the ratio between the intensities of reflected and incident beams. The specular reflectivity fulfils an additional condition of the reflected beam lying in the incident plane and the angles of reflectance and incidence being the same. It follows from this specification that 1) the direction of transferred momentum is orthogonal to the interface, and 2) structures lying in the plane perpendicular to \bar{q} are averaged, and consequently only this averaged structure along the bilayer normal has an impact on $R(q)$.

Neutrons enter a silicon block through a side and reach the Si/SiO₂ surface with deposited material. The SiO₂ layer with adhered lipid bilayers and water environment can be approximated as a system of layers (boxes) parallel with the Si/SiO₂ surface with constant SLDs. As it follows from the Schrödinger equation for the given geometry, each layer can be characterized by a refractive index

$$n = \sqrt{1 - \frac{\lambda^2}{\pi} \rho}, \quad (1)$$

where λ is the wavelength of the incident neutrons and ρ is the SLD of the layer. For systems composed of weakly absorbing nuclei, as it is for the samples investigated in the present paper, absorption can be neglected. At each interface a neutron wave is partly reflected back (into the same layer) and partly refracted or transmitted into an adjacent layer depending on their refractive indexes. Hence, including multiple reflections of neutron waves, models based on layered structures become fully dynamical. The final reflected beam from the whole system of layers can be calculated using basic optical principles.²³ In the current work we utilize the Parratt recursion relation,³⁵ in which the final reflectivity $R(q)$ of a stratified medium is calculated by a series of relations

$$\begin{aligned} R(q) &= \|X_N\|^2, \\ X_j &= e^{-i2k_j z_j} \frac{r_{j,j-1} + X_{j-1} e^{i2k_{j-1} z_j}}{1 + r_{j,j-1} X_{j-1} e^{i2k_{j-1} z_j}}, X_0 = 0, \\ r_{j,j-1} &= \frac{k_j - k_{j-1}}{k_j + k_{j-1}}, \\ k_j &= \sqrt{\frac{q^2}{4} - 4\pi(\rho_j - \rho_{Si})}, \end{aligned} \quad (2)$$

where j indexes layer interfaces from the last one marked with $j = 0$, preceded by the bulk water, to $j = N$ which labels the sample's entering interface at the silicon block. z_j is the position of j^{th} interface, k_j is the normal component of a wave vector in j^{th} layer with SLD ρ_j and ρ_{Si} is the SLD of a silicon block. The SLD profile is then partitioned along the bilayer normal into sections representing layers to which the Parratt formalism can be done applied.

Scattering density profile. As a model for the SLD profile of bilayer we used the component density model, which was originally proposed by Wiener and White³⁶ and later elaborated by Kučerka *et al.*^{24,25,31} for application in scattering experiments as the SDP model.

In this model a lipid molecule is divided into several component groups represented by their probability distributions along the bilayer normal. The components are: choline methyl groups, phosphate+CH₂CH₂N, carbonyl-glycerol (GC), hydrocarbon methylene groups (CH₂) and methyl groups of hydrocarbon chains (CH₃). In the current work, we slightly modified the SDP model to describe the whole choline group (choline methyl groups+CH₂CH₂N, CHO) and phosphate (PO) as two standalone component groups (Fig. 1). The reason is to utilize a possibility to suppress the contribution of phosphate groups on reflectivity curves and this way to enhance the resolution of polar headgroup regions. As it follows from the phosphate component volume data obtained by molecular dynamics simulations³⁷ the SLD of the phosphate group is about $4.0 \cdot 10^{-5} \text{ \AA}^{-2}$. Therefore, during the measurements we used also the contrast with similar SLD. The SLD profile of the bilayer is constructed through the so-called *primitive cell* of a bilayer, *i.e.* in analogy with crystallography, where the simplest repetitive region of a space forms the whole pattern. In our case the primitive cell is a volume containing a single lipid molecule in the form of a box. The area of its base corresponds to an important structure parameter - *interface area per lipid molecule A*. Each individual component inside the primitive cell is represented by its volume probability $v_j(z)$, which describes its probability to be found in the volume an infinitesimally thin layer in the position z perpendicular to the bilayer normal. One can easily construct the SLD profile of a bilayer from the component volume probabilities, while considering water molecules as an ideally filling background.²⁴ The SLD profile $\rho_{norm}(z)$ can be written as

$$\begin{aligned} \rho_{norm}(z) &= \left(1 - \sum_{j \neq HC} v_j(z)\right) \rho_w + \\ &+ \sum_{j \in HC} v_j(z) \rho_j + v_{CH_3} (\rho_{CH_3} - \rho_{CH_2}), \end{aligned} \quad (3)$$

COMMUNICATION

Journal Name

where HC denotes the hydrocarbon core region and index j comprises HC as well.

A special attention is paid to the methyl groups. They are located inside one layer together with methylene groups in the hydrocarbon core of the bilayer and therefore, following the same complementary principle as applied to other components and water background, they replace “methylene background” (ρ_{CH_2}).

Volume probabilities of components $v_i(z)$ are defined through the probability densities of components $p_i(z)$, describing the distributions of their volumes along the bilayer normal, component volumes V_i and A . Probability densities of methyl, carbonyl-glycerol, phosphate and choline groups are represented by Gaussians

$$p_i(z) = p_i(z; r_i, \sigma_i) = \frac{1}{\sqrt{2\pi\sigma_i^2}} \exp\left(-\frac{(z-r_i)^2}{2\sigma_i^2}\right), \quad (4)$$

where r_i is the mean position of i^{th} component and σ_i is the width of its probability density. For their volume probabilities along the normal holds the formula:

$$v_i(z) = \frac{p_i(z)}{A} V_i. \quad (5)$$

The region of the whole hydrocarbon chains (carbonyl groups excluded) is represented by the so-called *plateau-function*

$$p_i(z; r_{1i}, \sigma_{1i}, r_{2i}, \sigma_{2i}) = 0.5 \left(\operatorname{erf}\left(\frac{z-r_{1i}}{\sqrt{2}\sigma_{1i}}\right) - \operatorname{erf}\left(\frac{z-r_{2i}}{\sqrt{2}\sigma_{2i}}\right) \right), \quad (6)$$

$$\operatorname{erf}(x) = \frac{1}{\pi} \int_0^x e^{-t^2} dt,$$

where r 's denote the mean borders of hydrocarbon chains of a single lipid molecule (a single bilayer leaflet) and σ 's are their corresponding widths. From the widely accepted concept of an ideally filled bilayer hydrophobic region it follows for the hydrocarbon core/bilayer center that

$$v_{CH_2}(z_{center}) + v_{CH_3}(z_{center}) = v_{HC}(z_{center}) = 1. \quad (7)$$

In order to incorporate a presence of water molecules even inside the lipid leaflet, an additional parameter is introduced into the model in contrast to Wiener and White³⁶ and Kučerka *et al.*:^{5,24}

the rate of water in the bilayer leaflet, indexed by a and called further as *hydration* E_a . Then the SLD profile of a single leaflet on the normal is given by

$$\rho_{norm}(z) = \rho_W + \sum_a (1 - E_a) \left(\sum_i v_{i,a}(z) (\rho_i - \rho_W) + v_{CH_3,a}(z) (\rho_{CH_3} - \rho_{CH_2}) \right), \quad (8)$$

where a labels the present bilayer leaflets and i component groups in leaflet a . The SLD profile of a bilayer is obtained by adding two single leaflets together. To circumvent the

presence of voids in the hydrocarbon centre of a model bilayer, the corresponding positions and roughnesses of methylene regions in the bilayer centre are set equal. The methyl groups located in the bilayer center and belonging to different leaflets can be described by a common probabilistic and volumetric distribution. To incorporate the effect of different hydration of leaflets (E_1, E_2) within a bilayer, the volumetric distribution of methyl groups is multiplied by a factor $((1 - E_1) + (1 - E_2)) / 2$, in contrast to other components.

The molecular volumes of headgroup components and their distribution widths were taken as average values from the results of molecular dynamics simulations carried out by Klauda *et al.*³⁷ for different temperatures in the range 55 – 65 °C. This was allowed by a very small isobaric temperature expansion coefficient of a PC headgroup.³⁸ The component volumes of a methylene group V_{CH_2} at both measurement temperatures were from the work of Uhríková *et al.*³⁸ All mentioned component volumes are used as internal model parameters. For the volume of methyl component on the border of two primitive cells V_{CH_3} we used the fact that the volume of a single methyl group is ca double the size of the volume of a single methylene group³³ V_{CH_2} , hence $V_{CH_3} = 2V_{CH_2}$. The reason for setting up these parameters as fixed is the lack of small angle X-ray scattering data, which were used as complementary input in SDP model data analysis. The validity of this approach is supported by the results of similar experiments.^{7,10}

With the knowledge of hydrocarbon chain volumes V_C and the thickness of a complete hydrophobic core of a bilayer d_C one can directly connect the areas per lipid of leaflets in an asymmetric bilayer

$$A_2 = A_1 \frac{V_C}{A_1 d_C - V_C} \quad (9)$$

and decrease the number of free parameters, or, in the case of a symmetric bilayer ($A_1 = A_2$), even determine its value $A = 2V_C / d_C$ and completely exclude it from the system parameters. However, we found that a better practice is to artificially set the values of A 's to an expected values during the beginning of the fitting process and to release them or estimate them later, to avoid the strong influence of other parameters on their values.

A silicon block with a SiO_2 layer is incorporated into the model together with water as a part of an environment/matrix, into which a single bilayer or two bilayers are placed the same way as in the work of Kučerka *et al.*²⁴ The Si/SiO_2 interface is represented by an error function at $z = 0$ and the SiO_2 /water interface is represented by an error function with a variable position defining the thickness of an SiO_2 layer, thus the SLD profile of a background is

$$\rho_{env} = \rho_{Si} + 0.5 \left(1 + \operatorname{erf}\left(\frac{z}{\sqrt{2}\sigma_{Si}}\right) \right) (\rho_{SiO_2} - \rho_{Si}) + 0.5 \left(1 + \operatorname{erf}\left(\frac{z-r_{SiO_2}}{\sqrt{2}\sigma_{SiO_2}}\right) \right) (\rho_W - \rho_{SiO_2}), \quad (10)$$

Journal Name

where σ_{Si} represents the roughness of an Si/SiO₂ interface, r_{SiO_2} and σ_{SiO_2} are the position and the roughness of an SiO₂/water interface, respectively, and ρ 's are the SLDs of individual parts of the environment. Hence, the complete SLD profile along the normal is

$$\rho_{norm}(z) = \rho_{env} + \sum_j \left(\sum_{a \text{ in } j} (1 - E_a) \left[\sum_{i \text{ in } a} v_i(z) (\rho_i - \rho_w) + \frac{v_{CH_3, j}(z)}{2} (\rho_{CH_3} - \rho_{CH_2}) \right] \right) \quad (11)$$

where j labels bilayers, a leaflets within j^{th} bilayer and i labels component groups and regions within a^{th} leaflet. In this way a complete system of a single bilayer or the system of a floating bilayer is constructed in the framework of our SLD model and is transformed via Parratt's formalism consisting of 5 recursion layers per Angstrom (2) into a model reflectivity curve.

The model was applied to experimental reflectivity curves by minimization of

$$\chi^2 = \sum_{\text{exp. points}} \frac{(R_{model}(q_i) - R_{exp}(q_i))^2}{\sigma_i^2} \quad (12)$$

The resolution for each individual point was also included into the modelled reflectivity by convolution of $R(q)$ with the resolution function of the reflectometer $\Delta q(q)$.

Surface defects evaluation. A big difference between the modeling of vesicle bilayers and adsorbed bilayers is related to the presence of surface defects for the latter. Surface defects are represented in our model by the presence of hydration water in the hydrophobic core of the bilayer. Presence of water in this region strongly affects the values of other free parameters due to the significant space occupied by hydrocarbon chains. For this reason we devoted special attention to its evaluation during fitting process. E_a values were updated repeatedly by fitting all three scattering curves after each change of hydrocarbon region borders. After reaching a local minimum, we approached a model modification with asymmetrical leaflets hydration. Thus the extent of surface defects can be obtained individually per leaflet with a high relative precision. The previous step has high importance, especially for supported bilayers, where each leaflet undergoes different environment interactions.

Results and discussion

Supported bilayer

In the first step, the model was applied to the reflectivity curves of a supported bilayer consisting of diC22:0PC in three different contrasts, as commonly done for reflectometry studies in lipid bilayer systems. The experimental reflectivity curves are shown in Fig. 2A together with the fit curves. Fig. 2B shows the SLD profiles derived from the model as a function of the position along the bilayer normal. All three reflectivity

curves display a minimum between 0.12 and 0.15 Å⁻¹, which was found to be sensitive to the thickness of the bilayer as expected due to the interference of reflected waves from the top and the bottom of the bilayer.

The fitting process was divided into three parts. In the first step we kept the relative distance of each headgroup component from the hydrocarbon core constant in both leaflets. The area per lipid was also kept fixed at the value 60 Å², which is slightly higher than usual areas of lipids in the gel (L_β) phase.³³ Hence, only dominant regions were fitted – the SiO₂ layer and the hydrocarbon core sizes with the hydration of the bilayer. After the achievement of a local minimum, when further (realistic) fit improvement was not possible, different hydrations of bilayer leaflets were allowed and the positions of component groups in the headgroups were fitted under the condition of their symmetry with regard to hydrocarbon core borders. In the final step, area per lipid A in a combination with leaflet hydrations and individual asymmetrical component group positions were released and fitted repeatedly. The spread of normalized residual values $(R_{model}(q_i) - R_{exp}(q_i)) / \sigma_i$ was monitored to evaluate the goodness of the fitted curves. For the present case it always lies within the interval (-2, 2) for almost of all q -values.

In contrast to König *et al.*,³⁹ Charitat *et al.*⁴⁰ and Gutberlet *et al.*,¹⁷ where adsorbed PC bilayers were measured by SNR and Stidder *et al.*,⁴¹ where SNR was applied to supported dipalmitoylphosphatidylethanolamine (diC16:0PE) bilayers, we did not detect a bulk water layer between the SiO₂ surface layer and the adsorbed diC22:0PC bilayer. From the position of a choline group in the bilayer leaflet closer to the SiO₂ layer, we can deduce that the adsorbed bilayer is in a direct contact with the hydrated silicon oxide layer. This is not surprising, while in an agreement with other SNR results from recent experiments.^{42,43}

The structural parameters obtained by the analysis of the diC22:0PC bilayer according to the SDP model are summarized in Table 1.

The thickness of the hydrocarbon region is 44.9 ± 0.1 Å. If we suppose that the chain tilt of lipid bilayers in the gel phase does not depend on their length,³³ then using the value of the hydrocarbon thickness of, for example, diC14:0PC in the gel phase¹² $2D_C = 30.3$ Å², we can estimate $2D_C$ of a non-perturbed diC22:0PC bilayer to $2D_C = 47.6$ Å. Our value $2D_C = 44.9 \pm 0.1$ Å is lower, what can be explained by the interaction with the SiO₂ surface. On the other side, our $2D_C$ value is in a very good agreement with a similar estimation ($2D_C = 44.0$ Å) if the results of Charitat *et al.*⁴⁰ for diC16:0PC and diC18:0PC are used as reference.

The area per lipid of the leaflet in contact with the SiO₂ layer $A = 55 \pm 1$ Å² is slightly higher, but within the experimental accuracy, than that of the outer leaflet, which is in contact with bulk water, $A = 53 \pm 1$ Å². This might be caused by a different kind of environment interactions or by a different type of deposition (the lower leaflet was deposited by a vertical deposition while the outer leaflet by horizontal). This corresponds to the results of Charitat *et al.*⁴⁰ and Gutberlet *et al.*,¹⁷ where non-symmetrical box models were applied.

COMMUNICATION

Journal Name

We found that surface defects were present in the supported bilayers. As mentioned before, the extent of defects is evaluated by the amount of water detected in the hydrophobic core of the bilayer. The overall coverage of the silicon block, defined as a complement to unit hydration, was ca 90 % (89.5 ± 0.5 % and 91.2 ± 0.4 % for inner and outer leaflet respectively) (Table 1). The hydration of the lower leaflet core is slightly higher than the hydration of the outer one, but the difference is less than 2 %.

Floating bilayer

A d62-diC16:0PC bilayer floating over a supported diC22:0PC bilayer was measured in three different contrasts at 25 °C and 55 °C. The fitting process for the floating bilayer was similar to the procedure for the supported bilayer described above, while it was considered as completely symmetrical (component group positions, hydration, and hydrocarbon core roughnesses). As for the supported bilayer parameters, we varied only their relative position to the SiO₂ surface and their hydration, keeping the bilayer structure the same as obtained from the adsorbed diC22:0PC bilayer described in the previous section.

The best obtained model fit and its SLD profiles are shown in Fig. 3A and 3B. Our attempts to include the asymmetry in floating bilayer model or increased roughness to account for any effects coming from different depositions of its leaflets,

did not improve our fits significantly. Nevertheless, the hydrocarbon region thickness $2D_C = 35.9 \pm 0.5$ Å is higher than hydrocarbon region thickness of the same system in the same phase $2D_C = 34$ Å obtained by Charitat *et al.*⁴⁰ and $2D_C = 32.0 \pm 2$ Å obtained by Fragneto *et al.*⁴⁴ suggesting that structural differences may have been present.

At 55 °C we obtained a much better global fit. The fits with the corresponding SLD profiles are depicted in Fig. 4A and 4B. A change in the hydrocarbon region thickness, with respect to the value found at the lower temperature, was observed. This was expected since the gel-to-liquid phase transition temperature for d62-diC16:0PC is $T_m = 39$ °C. The hydrocarbon thickness we obtained $2D_C = 27.2 \pm 0.5$ Å is in a very good agreement with the thickness $2D_C = 27.9$ Å obtained by Kučerka *et al.*³¹ with a similar lipid bilayer model from small-angle neutron scattering on unilamellar vesicles. However, the region roughness in our case is significantly higher $\sigma_{CH_2} = 4.8 \pm 0.5$ Å than the value of Kučerka *et al.*³¹ $\sigma_{CH_2} = 2.5$ Å. This is probably caused by fluctuations arising from higher freedom of the floating bilayer in comparison to the bilayer in the form of a vesicle.

If we compare the estimated hydration of the floating bilayer at 25 °C and its value at 55 °C, we can see that it was decreased by more than 15 %. This leads to conclusion that the fluid phase is more suitable for the

Table 2: The obtained values of the bilayer model structure parameters for a supported diC22:0PC bilayer and a floating d62-diC16:0PC bilayer at 25 °C and 55 °C. For diC22:0PC area per lipid the first and the second number represent the area per lipid in the first and in the second leaflet in z-direction, respectively. The same applies for hydrations E_i . The asterisk (*) denotes the position values obtained with fixed relative positions of component groups and equal to ones obtained by Kučerka *et al.*²⁴ For floating bilayers the hydration in parentheses denotes the average hydration of the supported bilayer. The errors were obtained by iterative fitting refinements of parameters in groups of two or three. The double asterisk (**) in the last column denotes recalculated diC16:0PC bilayer structure parameters obtained by Kučerka *et al.*²⁴ from SANS on unilamellar vesicles.

Free parameter	diC22:0PC	d62-diC16:0PC at 25 °C	d62-diC16:0PC at 55 °C	diC16:0PC** at 66 °C
σ_{Si} [Å]	4.2 ± 0.3	4.1 ± 0.2	4.1 ± 0.2	-
r_{SiO_2/H_2O} [Å]	14.0 ± 0.1	13.7 ± 0.1	13.7 ± 0.1	-
σ_{SiO_2} [Å]	3.0 ± 0.5	3.7 ± 0.2	3.7 ± 0.2	-
A [Å ²]	55 ± 1 53 ± 1	64.4 ± 0.3	66.6 ± 0.2	65.0
E_i	0.105 ± 0.005 0.088 ± 0.004	0.443 ± 0.001 (0.171 ± 0.001)	0.291 ± 0.001 (0.159 ± 0.004)	-
$r_{CHO,1}$ [Å]	18.7 ± 0.6	103.3*	101.4 ± 0.4	104.3
$r_{PO,1}$ [Å]	20.2 ± 1.0	106.8*	104.3 ± 0.7	105.1
$r_{GC,1}$ [Å]	23.0 ± 0.5	113.6*	108.7 ± 0.4	109.3
$r_{CH_2,1}$ [Å]	25.3 ± 0.5	115.2 ± 0.5	110.0 ± 0.5	110.0
$\sigma_{CH_2,1}$ [Å]	2.8 ± 0.6	2.9 ± 0.5	4.8 ± 0.5	2.5
$r_{CH_2,2}$ [Å]	70.2 ± 0.5	151.1 ± 0.5	137.2 ± 0.5	137.9
$\sigma_{CH_2,2}$ [Å]	2.2 ± 0.6	2.9 ± 0.5	4.8 ± 0.5	2.5
$r_{GC,2}$ [Å]	71.3 ± 0.5	152.7*	138.4 ± 0.4	138.7
$r_{PO,2}$ [Å]	74.8 ± 1.6	159.4*	142.8 ± 0.7	142.9
$r_{CHO,2}$ [Å]	75.4 ± 0.4	163.0*	145.7 ± 0.4	143.7

reorganization of lipid molecules into well-ordered bilayer than the gel phase.

If we assign $r_{CHO,2} + \sigma_{CHO}$ and $r_{CHO,1} - \sigma_{CHO}$ as the outer border of the supported bilayer and the lower border of the floating bilayer, respectively, we can estimate the interbilayer water thickness D_w . Between its estimated value from the data at 25 °C $D_w = 22.4$ Å and the value obtained from the data at 55 °C $D_w = 20.5$ Å is the difference of ca. 2 Å. Albeit the validity of this approximation is strongly dependent on which experimental technique is applied, the tendency agrees with a formerly observed behaviour of diC16:0PC bilayers across their main phase transition.²⁰

The interface area per lipid molecule $A = 66.6 \pm 0.2$ Å² in the floating bilayer at 55 °C is slightly higher than its value

obtained by Kučerka *et al.*,³¹ but the difference in the number of water molecules intercalated into the hydrophilic bilayer region per lipid molecule is less than 1 molecule. If we use the same definition for the bilayer borders as mentioned above and the total phosphatidylcholine headgroup volume, given as the sum of volumes of its components, we can estimate the average number of water molecules in the floating bilayer hydrophilic region per one lipid molecule to $N_w = 14.4$.

The arrangement of component groups in the hydrophilic regions differs slightly from the arrangement obtained by Kučerka *et al.*³¹ Firstly, the difference between the positions of the carbonyl-glycerol group is 0.5 Å shifted outwards from the hydrocarbon core in our case. Similar shifts can be seen also for the phosphate and the choline groups. As the shift

COMMUNICATION

Journal Name

increases with the distance from the hydrocarbon core, we assume that they are predominantly caused by the bilayer undulations. There is also the effect of different component specifications in the case of phosphate and choline groups, when one compares our bilayer model with that of Kučerka *et al.*,^{24,31} but as it can be seen in the results of Heberle *et al.*,⁹ the shift is around 1 Å. Hence we consider bilayer undulations as the main reason for a wider spread of headgroup components along the bilayer normal.

Conclusions

The modified SDP model was applied successfully to the analysis of neutron reflectivity from both supported and floating bilayers. The effect of disorder after deposition was suppressed by heating the bilayer into the liquid phase. In both cases, for a supported bilayer as well as a floating bilayer in the fluid phase, the SLD profile model revealed their internal structure in terms of hydrocarbon core region, headgroup components and hydration.

The applied model is based on the model originally elaborated for simultaneous evaluation of small-angle X-ray and neutron scattering data, whereas in our case we used only data obtained by SNR. This fact is taken into consideration by the decreased number of free parameters of our model. The original SDP model is parameterized by 14 independent parameters per bilayer with 4 additional constraints. In our case, a supported asymmetric bilayer is modeled by 13 free parameters, whereas a floating bilayer by only 6 free parameters. This allowed us to obtain a robust model converging repeatedly to the same minima.

In the case of a supported diC22:OPC bilayer results showed a slightly asymmetrical structure in the hydration of its leaflets, the leaflet interface areas per lipid molecule and the structure of its hydrophilic regions.

For the floating d62-diC16:OPC bilayer in the gel phase at 25 °C only its full thickness and average hydration were estimated. A more detailed analysis was not possible very likely because of the disorder present in the sample before the thermal annealing.

The contrast varied reflectivity curves of the floating d62-diC16:OPC bilayer in the fluid phase at 55 °C were fitted simultaneously with success by the applied model. The results display a symmetrical structure and lower hydration in comparison to its state in the gel phase after deposition. The mean positions of component groups in hydrophilic regions were shifted from the bilayer center increasingly with their relative distances from the bilayer center in comparison to the same bilayer structure obtained from small-angle neutron scattering on bilayers in the form of unilamellar vesicles. Moreover, the roughness of its hydrocarbon region was about twice the roughness in unilamellar vesicles. On the other side the mean thickness of the hydrocarbon region was in a very good agreement with small-angle neutron measurements. If we assume that the hydrocarbon core thickness does not depend on the curvature of undulations and that the average rate of the floating bilayer fluctuations is the same over any

coherently reflecting part of the floating bilayer, we can conclude that the floating bilayer fluctuates due to its freedom at higher rate than the bilayer in unilamellar vesicles.

These results show that the system is appropriate as biomembrane model. It has been found previously that when both bilayers in a double bilayer system are brought to the fluid phase, there is considerable mixing of the lipids from the two bilayers.^{42,45} By using a longer chain lipid (diC22:OPC) as supporting bilayer this stays the gel phase and there is no mixing with the floating one. The system represents therefore a step forward the preparation of complex model membrane systems for structural studies of the floating bilayer.

Acknowledgements

This work was supported by the VEGA 1/0534/15 grant and JINR 04-4-1121-2015/2017 project. PB thanks the Comenius University Science Park supported by the Research and Development Operational Programme funded by the ERDF Grant number ITMS 26240220086. We acknowledge the use of the preparation and characterization tools provided by the Partnership for Soft Condensed Matter (PSCM) at ILL. MB also thanks the Central European Neutron Initiative for a one-year scholarship and the staff of Large Scales Structure Group in Institute Laue-Langevin for help, discussions and hospitality.

References

- 1 T. Heimburg, *Thermal Biophysics of Membranes*, Wiley-VCH Verlag, Weinheim, 2007.
- 2 J. Daillant, E. Bellet-Amalric, A. Braslau, T. Charitat, G. Fragneto, F. Graner, S. Mora, F. Rieutord and B. Stidder, *Proc. Natl. Acad. Sci. U. S. A.*, 2005, **102**, 11639–11644.
- 3 M. J. Hope, M. B. Bally, L. D. Mayer, A. S. Janoff and P. R. Cullis, *Chem. Phys. Lipids*, 1986, **40**, 89–107.
- 4 R. C. MacDonald, R. I. MacDonald, B. P. M. Menco, K. Takeshita, N. K. Subbarao and L. Hu, *Biochim. Biophys. Acta*, 1991, **1061**, 297–303.
- 5 M.-P. Nieh, N. Kučerka and J. Katsaras, *Meth. Enzymol.*, 2009, **465**, 3–20.
- 6 J. Gallová, D. Uhríková, A. Islamov, A. Kuklin and P. Balgavy, *Gen. Physiol. Biophys.*, 2004, **23**, 113–128.
- 7 J. Pan, S. Tristram-Nagle, N. Kučerka and J. F. Nagle, *Biophys. J.*, 2008, **94**, 117–124.
- 8 M. Klacsová, M. Bulacu, N. Kučerka, D. Uhríková, J. Teixeira, S. J. Marrink and P. Balgavý, *Biochim. Biophys. Acta*, 2011, **1808**, 2136–2146.
- 9 F. A. Heberle, J. Pan, R. F. Standaert, P. Drazba, N. Kučerka and J. Katsaras, *Eur. Biophys. J.*, 2012, **41**, 875–890.
- 10 P. Heftberger, B. Kollmitzer, F. A. Heberle, J. Pan, M. Rappolt, H. Amenitsch, N. Kučerka, J. Katsaras and G. Pabst, *J. Appl. Crystallogr.*, 2014, **47**, 173–180.
- 11 J. Katsaras, D. S. Yang and R. M. Epand, *Biophys. J.*, 1992, **63**, 1170–1175.
- 12 S. Tristram-Nagle, Y. Liu, J. Legleiter and J. F. Nagle, *Biophys. J.*, 2002, **83**, 3324–3335.
- 13 P. Balgavý, D. Uhríková, J. Gallová, K. Lohner and G. Degovics, in *Trends in colloid and interface science VII*, eds. P. Laggner and O. Glatter, Steinkopff, 1993, pp. 184–185.

Journal Name

- 14 J. Karlovská, K. Lohner, G. Degovics, I. Lacko, F. Devínsky and P. Balgavý, *Chem. Phys. Lipids*, 2004, **129**, 31–41.
- 15 T. A. Harroun, D. Marquardt, J. Katsaras and J. Atkinson, *J. Phys. Conf. Ser.*, 2010, **251**, 012039.
- 16 E. Sackmann, *Science*, 1996, **271**, 43–48.
- 17 T. Gutberlet, R. Steitz, G. Fragneto and B. Klösgen, *J. Phys. Condens. Matter*, 2004, **16**, S2469.
- 18 H. P. Vacklin, F. Tiberg, G. Fragneto and R. K. Thomas, *Langmuir*, 2005, **21**, 2827–2837.
- 19 G. Fragneto, T. Charitat, F. Graner, K. Mecke, L. Perino-Gallice and E. Bellet-Amalric, *Europhys. Lett.*, 2001, **53**, 100–106.
- 20 G. Fragneto, T. Charitat and J. Daillant, *Eur. Biophys. J.*, 2012, **41**, 863–874.
- 21 A. V. Hughes, J. R. Howse, A. Dabkowska, R. A. L. Jones, M. J. Lawrence and S. J. Roser, *Langmuir*, 2008, **24**, 1989–1999.
- 22 W. T. Heller, *Acta Crystallogr. D*, 2010, **66**, 1213–1217.
- 23 M. Born and E. Wolf, *Principles of optics: electromagnetic theory of propagation, interference and diffraction of light*, Cambridge University Press, Cambridge, 1999.
- 24 N. Kučerka, J. F. Nagle, J. N. Sachs, S. E. Feller, J. Pencer, A. Jackson and J. Katsaras, *Biophys. J.*, 2008, **95**, 2356–2367.
- 25 N. Kučerka, J. Gallová, D. Uhríková, P. Balgavý, M. Bulacu, S.-J. Marrink and J. Katsaras, *Biophys. J.*, 2009, **97**, 1926–1932.
- 26 N. Kučerka, B. W. Holland, C. G. Gray, B. Tomberli and J. Katsaras, *J. Phys. Chem. B*, 2011, **116**, 232–239.
- 27 P. Shekhar, H. Nanda, M. Lösche and F. Heinrich, *Journal Of Applied Physics*, 2011, **110**, 102216.
- 28 M. C. Wiener, R. M. Suter and J. F. Nagle, *Biophys. J.*, 1989, **55**, 315–325.
- 29 J. Katsaras, *J. Phys. Chem.*, 1995, **99**, 4141–4147.
- 30 J. F. Nagle and S. Tristram-Nagle, *Biochim. Biophys. Acta*, 2000, **1469**, 159–195.
- 31 N. Kučerka, M.-P. Nih and J. Katsaras, *Biochim. Biophys. Acta*, 2011, **1808**, 2761–2771.
- 32 R. Cubitt and G. Fragneto, *Appl. Phys. A*, 2002, **74**, 329–331.
- 33 D. Marsh, *Handbook of Lipid Bilayers*, CRC Press, Boca Raton, 2nd edn., 2013.
- 34 D. Richard, M. Ferrand and G. J. Kearley, *J. Neutron Res.*, 1996, **4**, 33–39.
- 35 L. G. Parratt, *Phys. Rev.*, 1954, **95**, 359–369.
- 36 M. C. Wiener and S. H. White, *Biophys. J.*, 1992, **61**, 434–447.
- 37 J. B. Klauda, N. Kučerka, B. R. Brooks, R. W. Pastor and J. F. Nagle, *Biophys. J.*, 2006, **90**, 2796–2807.
- 38 D. Uhríková, P. Rybár, T. Hianik and P. Balgavý, *Chem. Phys. Lipids*, 2007, **145**, 97–105.
- 39 B. W. König, S. Krueger, W. J. Orts, C. F. Majkrzak, N. F. Berk, J. V. Silverton and K. Gawrisch, *Langmuir*, 1996, **12**, 1343–1350.
- 40 T. Charitat, E. Bellet-Amalric, G. Fragneto and F. Graner, *Eur. Phys. J. B*, 1999, **8**, 583–593.
- 41 B. Stidder, G. Fragneto and S. J. Roser, *Soft Matter*, 2007, **3**, 214–222.
- 42 Y. Gerelli, L. Porcar and G. Fragneto, *Langmuir*, 2012, **28**, 15922–15928.
- 43 Y. Gerelli, L. Porcar, L. Lombardi and G. Fragneto, *Langmuir*, 2013, **29**, 12762–12769.
- 44 G. Fragneto, T. Charitat, E. Bellet-Amalric, R. Cubitt and F. Graner, *Langmuir*, 2003, **19**, 7695–7702.
- 45 V. Rondelli, E. Del Favero, S. Motta, L. Cantù, G. Fragneto and P. Brocca, *European Physical Journal E*, 2013, **36**.

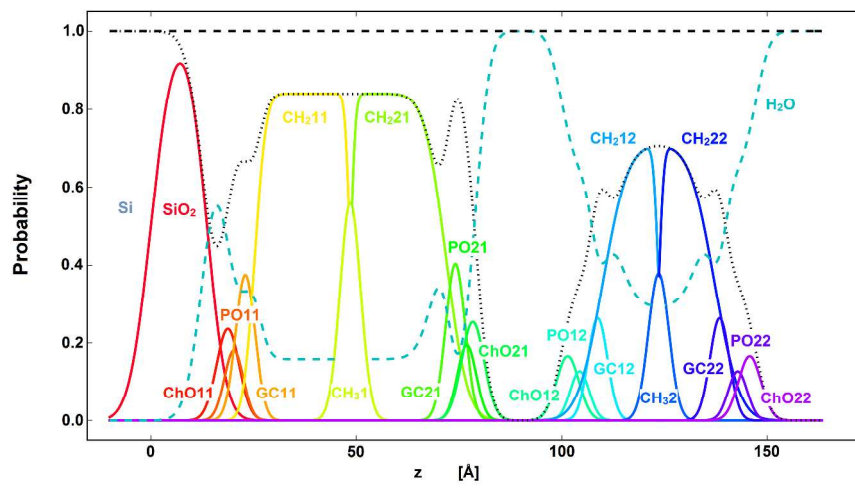
Figure captions

Fig. 1: Scheme of component group volumetric probabilities within the SLD profile model of supported and floating bilayers. Individual components depict distinct regions (a silicon layer - Si, a silicon dioxide layer - SiO₂, leaflet hydrocarbon chain region CH₂XY, water - H₂O) and molecular component groups (choline - ChOXY, phosphate - POXY, carbonyl-glycerol - GCXY, methyl groups - CH₃Y). The first and second numbers in the group names label the leaflet and the bilayer respectively.

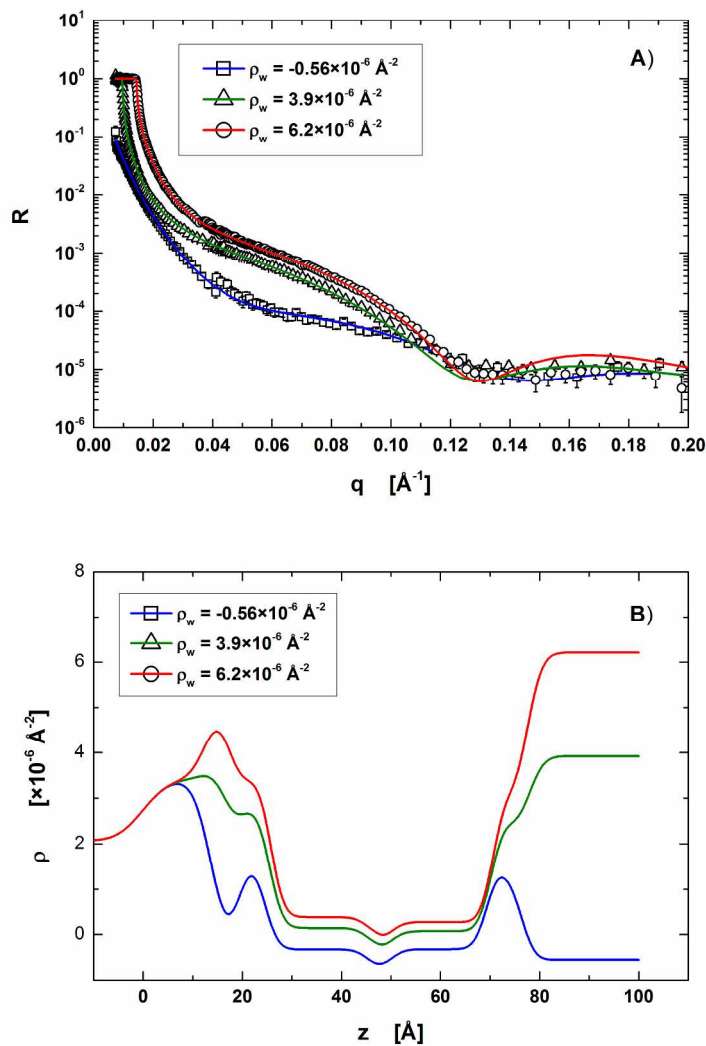
Fig. 2: (A) The normalized reflectivity curves of a supported diC22:0PC bilayer on the hydrophilic surface of a silicon substrate. The bilayer was measured in three different contrasts: pure H₂O (squares, blue line), mixture of H₂O/D₂O (triangles, green line) and in pure D₂O (circles, red line). The lines represent the best simultaneous fit of the component bilayer model to the data. (B) The corresponding SLD profiles. The lines represent the bilayer model in three different contrasts and correspond to the fitting lines.

Fig. 3: (A) The normalized reflectivity curves of d62-diC16:0PC bilayer floating over a diC22:0PC bilayer at 25 °C in three different contrasts. The lines represent the best simultaneous fit of the component bilayer model to the data. (B) The corresponding SLD profiles.

Fig. 4: (A) The normalized reflectivity curves of a floating d62-diC16:0PC bilayer over a diC22:0PC bilayer at 55 °C in three different contrasts. The lines represent the best simultaneous fit of the component bilayer model to the data. (B) The corresponding SLD profiles.

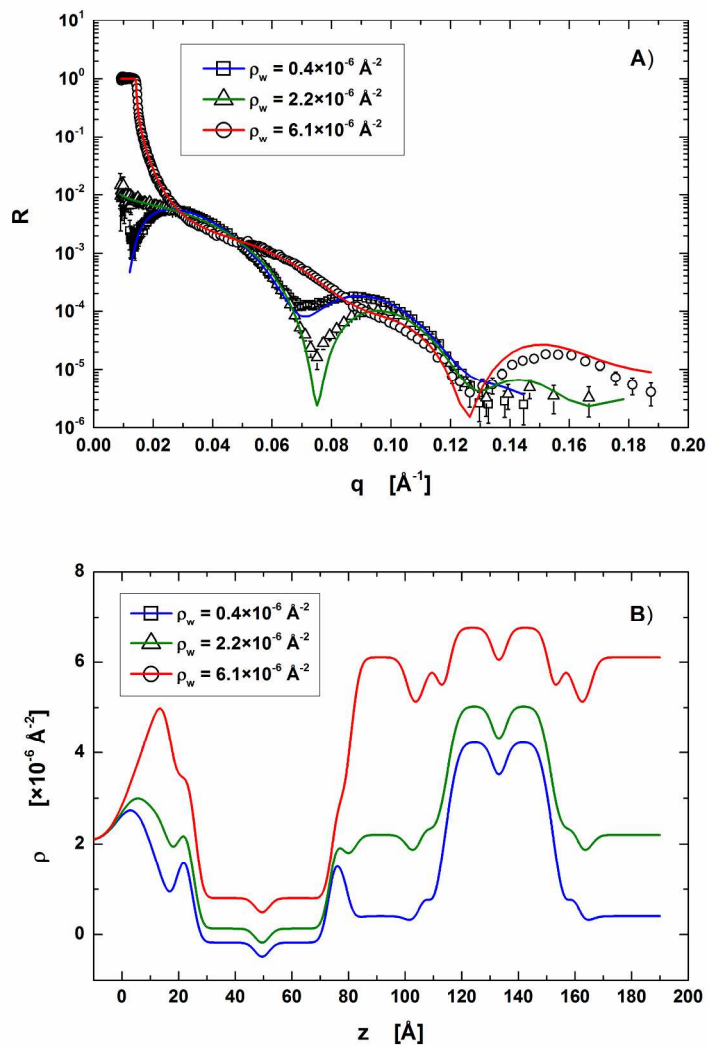


1603x796mm (96 x 96 DPI)

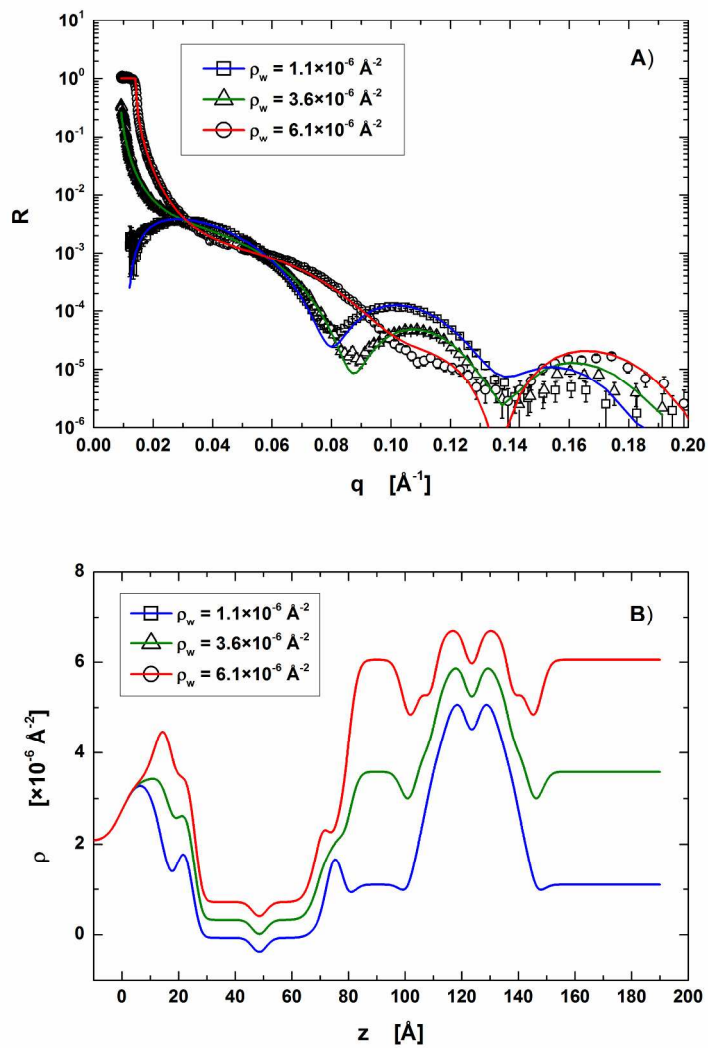


(A) The normalized reflectivity curves of a supported diC22:0PC bilayer on the hydrophilic surface of a silicon substrate. The bilayer was measured in three different contrasts: pure H₂O (squares, blue line), mixture of H₂O/D₂O (triangles, green line) and in pure D₂O (circles, red line). The lines represent the best simultaneous fit of the component bilayer model to the data. (B) The corresponding SLD profiles. The lines represent the bilayer model in three different contrasts and correspond to the fitting lines.

117x165mm (600 x 600 DPI)



(A) The normalized reflectivity curves of d62-diC16:0PC bilayer floating over a diC22:0PC bilayer at 25 °C in three different contrasts. The lines represent the best simultaneous fit of the component bilayer model to the data. (B) The corresponding SLD profiles.
117x165mm (600 x 600 DPI)



(A) The normalized reflectivity curves of a floating d62-diC16:0PC bilayer over a diC22:0PC bilayer at 55 °C in three different contrasts. The lines represent the best simultaneous fit of the component bilayer model to the data. (B) The corresponding SLD profiles.
117x165mm (600 x 600 DPI)